

Electronic Supplementary Information for

Rare earth induced formation of $\delta\text{-BiB}_3\text{O}_6$ at ambient pressure with strong second harmonic generation

Rihong Cong,^{a,b} Tao Yang,^b Zheshuai Lin,^{c} Lei Bai,^c Jing Ju,^a Fuhui Liao,^a Yingxia Wang,^{*a} Jianhua Lin^{*a}*

^aBeijing National Laboratory for Molecular Sciences, State Key Laboratory of Rare Earth Materials Chemistry and Applications, College of Chemistry and Molecular Engineering, Peking University, Beijing 100871, P. R. China

^bCollege of Chemistry and Chemical Engineering, Chongqing University, Chongqing 400044, P. R. China

^cTechnical Institute of Physics and Chemistry, Chinese Academy of Science, P.O. Box 2711, Beijing 100080, P. R. China

*Correspondence authors, Email: wangyx@pku.edu.cn, zslin@mail.ipc.ac.cn, and jhlin@pku.edu.cn; Tel: (8610)62755538, Fax: (8610)62753541.

SHG calculated method and real-space atom-cutting technique. As early in 1963, the formalism to calculate SHG coefficients based on band structure was proposed [1]. However, due to the difficulty in dealing with the explicit divergence in the static limit of their formula, the calculation was not practical until the 1990s when some groups [2-6] greatly improved the evaluation methods. We made further improvement on the static SHG formula and eliminate the terms that may cause divergence [7,8], i.e., the SHG coefficient $\chi^{\alpha\beta\gamma}$ is expressed as:

$$\chi^{\alpha\beta\gamma} = \chi^{\alpha\beta\gamma}(\text{VE}) + \chi^{\alpha\beta\gamma}(\text{VH}) + \chi^{\alpha\beta\gamma}(\text{twobands}) \quad (\text{S1})$$

where $\chi^{\alpha\beta\gamma}(\text{VE})$ and $\chi^{\alpha\beta\gamma}(\text{VH})$ devote the contributions from virtual-electron processes and virtual-hole processes, respectively, and $\chi^{\alpha\beta\gamma}(\text{twobands})$ devote the contribution to $\chi^{(2)}$ from two band processes. The formulae for calculating $\chi^{\alpha\beta\gamma}(\text{VE})$, $\chi^{\alpha\beta\gamma}(\text{VH})$ and $\chi^{\alpha\beta\gamma}(\text{twobands})$ are given as follows:

$$\chi^{\alpha\beta\gamma}(\text{VH}) = \frac{e^3}{2\hbar^2 m^3} \sum_{vv'c} \int \frac{d^3 k}{4\pi^3} P(\alpha\beta\gamma) \text{Im}[p_{vv'}^\alpha p_{v'c}^\beta p_{cv}^\gamma] \left(\frac{1}{\omega_{cv}^3 \omega_{v'c}^2} + \frac{2}{\omega_{vc}^4 \omega_{cv'}^1} \right) \quad (\text{S2})$$

$$\chi^{\alpha\beta\gamma}(\text{VE}) = \frac{e^3}{2\hbar^2 m^3} \sum_{vc'c} \int \frac{d^3 k}{4\pi^3} P(\alpha\beta\gamma) \text{Im}[p_{vc}^\alpha p_{cc'}^\beta p_{c'v}^\gamma] \left(\frac{1}{\omega_{cv}^3 \omega_{vc'}^2} + \frac{2}{\omega_{vc}^4 \omega_{c'v}^1} \right) \quad (\text{S3})$$

$$\chi(\text{Two Bands}) = \frac{e^3}{\hbar^2 m^3} \sum_{vc} \int \frac{d^3 k}{4\pi^3} P(\alpha\beta\gamma) \frac{\text{Im}[p_{vc}^\alpha p_{cv}^\beta (p_{vv}^\gamma - p_{cc}^\gamma)]}{\omega_{vc}^5} \quad (\text{S4})$$

Here, α , β and γ are Cartesian components, v and v' denote valence bands, and c and c' denote conduction bands. $P(\alpha\beta\gamma)$ denotes full permutation and explicitly shows the Kleinman symmetry of the SHG coefficients. The band energy difference and momentum matrix elements are denoted as $\hbar\omega_{ij}$ and p_{ij}^α , respectively, and they are all implicitly k dependent.

It is well known that the band gap calculated by the local density approximation is in general smaller than the experimental data. This error is due to the discontinuity of exchange-correlation energy. Therefore, a scissors operator [9, 10] is usually introduced to shift all the conduction bands in order to agree with the measured value of the band gap. Assuming that the r_{mn} matrix elements are unchanged, the

momentum matrix elements should be renormalized regarding the change of the Hamiltonian in a way given by [11]

$$p_{nm} \rightarrow p_{nm} \frac{\omega_{nm} + \Delta/\hbar(\delta_{nc} - \delta_{mc})}{\omega_{nm}} \quad (11)$$

where the subscript *c* in the Kroneckers represents conduction band, and the ($\delta_{nc} - \delta_{mc}$) factor restricts the correction to pairs of bands only involving one valence and one conduction-band state.

To analyze the contribution of an ion (or cluster) to the *n*-th order susceptibility $\chi^{(n)}$, we present a model called the real-space atom-cutting method. In the calculation we divide the real space into individual zones, each of which contains an ion. For simplicity, we define the zones to be spheres centered on a specific ion. When we set the band wave function to zero in the zones that belong to a specific ion (which we refer to as “cutting”), the contribution of the ion is assumed to be cut away. Therefore, the contribution of an ion is extracted when we cut other ions from the total wave functions. For example, if the contribution of ion A to the *n*th-order susceptibility is denoted as $\chi_A^{(n)}$ (A), we can obtain it by cutting all ions except A from the original wave functions, i. e.,

$$\chi_A^{(n)} = \chi_{\text{All ions expt A are cut}}^{(n)} \quad (13)$$

The definition of the boundary of two nearest ions is given by the points at which the charge density in real space reaches a local minimum. By this strategy, the cutting radius of two nearest ions can be determined. The real-space atom-cutting method allows us to calculate the optical coefficients of cations or anionic groups separately. It is because that the overlap of wave functions between cations and anionic groups is very small, and the dipole transition between off-site atoms is much smaller than that of intra-atomic transitions, so its contribution to the optical response can be neglected in the first-order approximation. The validity of the real-space atom-cutting technique has been stringently tested in many NLO crystals [12].

[1] P. N. Butcher and T. P. McLean, Proc Phys Soc London **81**, 219 (1963).

- [2] D. E. Aspnes, Phys. Rev. B**6**, 4648 (1972).
- [3] E. Ghahramani, D. J. Moss and J. E. Sipe, Phys. Rev B**43**, 8990 (1990).
- [4] J. E. Sipe and E. Ghahramani, Phys. Rev. B**48**, 11705 (1993).
- [5] C. Aversa and J. E. Sipe, Phys. Rev. B **52**, 14632 (1995).
- [6] S. N. Rashkeev, W. R. L. Laambrecht and B. Segall, Phys. Rev. B**57**, 3905 (1998).
- [7] J. Lin, M. H. Lee, Z. P. Liu, C. T. Chen and C. J. Picard, Phys Rev B**60**, 13380 (1999).
- [8] Z. S. Lin, J. Lin, Z. Z. Wang, Y. C. Wu, N. Ye, C. T. Chen, R. K. Li, J. Phys. Condens. Matt. 2001, 13, R369-R384.
- [9] R. W. Godby, M. Schluter and L. J. Sham, Phys. Rev. B 1988, **37**, 10159.
- [10] C. S. Wang, and B. M. Klein, Phys. Rev. B**24**, 3417 (1981); M. S. Hybertsen and S. G. Louie, ibid. **34**, 5390 (1986).
- [11] Z. H. Levine and D. C. Allan, Phys. Rev. B**43**, 4187 (1991); J. L. P. Hughes and J. E. Sipe, ibid. **53**, 10751 (1996).
- [12] C. T. Chen, Z. S. Lin, Z. Z. Wang, Appl. Phys. B, 2004, 80, 1-25.

Table S1. The refined results of cell lattice parameters by Le Bail fitting of $\delta\text{-Bi}_{1-x}\text{RE}_x\text{B}_3\text{O}_6$ powder samples ($\text{RE} = \text{La, Ce, Pr, Nd}$, $x \leq 0.15$) obtained by sol-gel method.

Composition	a (Å)	b (Å)	c (Å)	V (Å ³)
$\delta\text{-Bi}_{0.990}\text{La}_{0.010}\text{B}_3\text{O}_6$	18.447	4.4492	4.2792	351.23
$\delta\text{-Bi}_{0.975}\text{La}_{0.025}\text{B}_3\text{O}_6$	18.446	4.4493	4.2800	351.26
$\delta\text{-Bi}_{0.950}\text{La}_{0.050}\text{B}_3\text{O}_6$	18.444	4.4498	4.2799	351.27
$\delta\text{-Bi}_{0.925}\text{La}_{0.075}\text{B}_3\text{O}_6$	18.442	4.4504	4.2808	351.34
$\delta\text{-Bi}_{0.900}\text{La}_{0.100}\text{B}_3\text{O}_6$	18.442	4.4510	4.2819	351.48
$\delta\text{-Bi}_{0.875}\text{La}_{0.125}\text{B}_3\text{O}_6$	18.440	4.4519	4.2828	351.59
$\delta\text{-Bi}_{0.850}\text{La}_{0.150}\text{B}_3\text{O}_6$	18.442	4.4528	4.2834	351.74
$\delta\text{-Bi}_{0.990}\text{Ce}_{0.010}\text{B}_3\text{O}_6$	18.446	4.4488	4.2788	351.15
$\delta\text{-Bi}_{0.975}\text{Ce}_{0.025}\text{B}_3\text{O}_6$	18.445	4.4489	4.2791	351.15
$\delta\text{-Bi}_{0.950}\text{Ce}_{0.050}\text{B}_3\text{O}_6$	18.444	4.4492	4.2795	351.19
$\delta\text{-Bi}_{0.925}\text{Ce}_{0.075}\text{B}_3\text{O}_6$	18.446	4.4496	4.2799	351.27
$\delta\text{-Bi}_{0.900}\text{Ce}_{0.100}\text{B}_3\text{O}_6$	18.443	4.4500	4.2807	351.33
$\delta\text{-Bi}_{0.875}\text{Ce}_{0.125}\text{B}_3\text{O}_6$	18.443	4.4504	4.2811	351.39
$\delta\text{-Bi}_{0.850}\text{Ce}_{0.150}\text{B}_3\text{O}_6$	18.444	4.4509	4.2814	351.47
$\delta\text{-Bi}_{0.990}\text{Pr}_{0.010}\text{B}_3\text{O}_6$	18.436	4.4482	4.2796	350.96

$\delta\text{-Bi}_{0.975}\text{Pr}_{0.025}\text{B}_3\text{O}_6$	18.440	4.4483	4.2788	350.98
$\delta\text{-Bi}_{0.950}\text{Pr}_{0.050}\text{B}_3\text{O}_6$	18.434	4.4488	4.2796	350.97
$\delta\text{-Bi}_{0.925}\text{Pr}_{0.075}\text{B}_3\text{O}_6$	18.436	4.4490	4.2798	351.04
$\delta\text{-Bi}_{0.900}\text{Pr}_{0.100}\text{B}_3\text{O}_6$	18.434	4.4492	4.2803	351.05
$\delta\text{-Bi}_{0.875}\text{Pr}_{0.125}\text{B}_3\text{O}_6$	18.444	4.4489	4.2792	351.14
$\delta\text{-Bi}_{0.850}\text{Pr}_{0.150}\text{B}_3\text{O}_6$	18.449	4.4491	4.2794	351.26
$\delta\text{-Bi}_{0.990}\text{Nd}_{0.010}\text{B}_3\text{O}_6$	18.448	4.4492	4.2790	351.23
$\delta\text{-Bi}_{0.975}\text{Nd}_{0.025}\text{B}_3\text{O}_6$	18.442	4.4485	4.2786	351.02
$\delta\text{-Bi}_{0.950}\text{Nd}_{0.050}\text{B}_3\text{O}_6$	18.439	4.4483	4.2791	350.97
$\delta\text{-Bi}_{0.925}\text{Nd}_{0.075}\text{B}_3\text{O}_6$	18.434	4.4482	4.2789	350.87
$\delta\text{-Bi}_{0.900}\text{Nd}_{0.100}\text{B}_3\text{O}_6$	18.430	4.4475	4.2790	350.73
$\delta\text{-Bi}_{0.875}\text{Nd}_{0.125}\text{B}_3\text{O}_6$	18.436	4.4472	4.2774	350.69
$\delta\text{-Bi}_{0.850}\text{Nd}_{0.150}\text{B}_3\text{O}_6$	18.427	4.4468	4.2781	350.55

Table S2 Crystallographic parameters from literatures: *J. S. Knyrim, P. Becker, D. Johrendt, H. Huppertz, Angew. Chem. Int. Ed. 2006, 45, 8239-8241; H. Emme, C. Despotopoulou, H. Huppertz, Z. Anorg. Allg. Chem., 2004, 630, 2450-2457.*

Composition	<i>a</i> (Å)	<i>b</i> (Å)	<i>c</i> (Å)	<i>V</i> (Å ³)	Method
$\delta\text{-BiB}_3\text{O}_6$	18.448(4)	4.4495(9)	4.2806(9)	351.4(2)	Single crystal XRD
$\delta\text{-LaB}_3\text{O}_6$	18.482(5)	4.4781(7)	4.308(2)	356.55(9)	Powder XRD
$\delta\text{-CeB}_3\text{O}_6$	18.442(9)	4.461(2)	4.294(2)	354.2(2)	Single crystal XRD
$\delta\text{-PrB}_3\text{O}_6$	18.381(6)	4.4464(7)	4.278(2)	349.6(2)	Powder XRD
$\delta\text{-NdB}_3\text{O}_6$	18.348(7)	4.4394(8)	4.272(2)	348.0(2)	Powder XRD

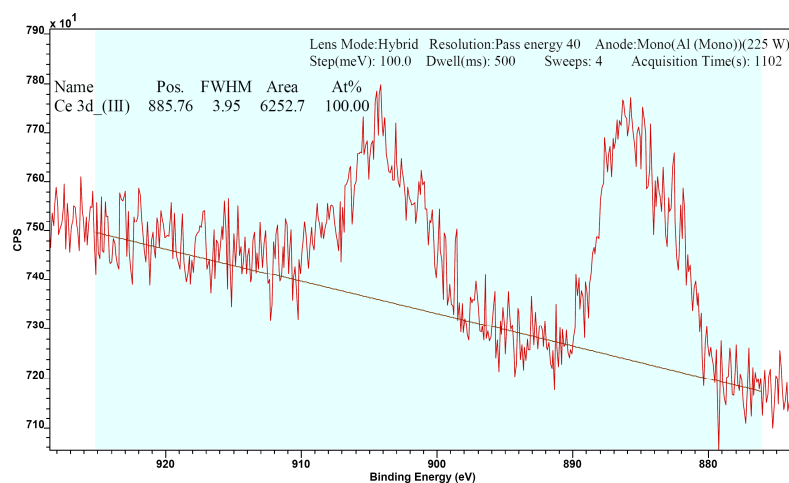


Figure S1. X-ray photoelectron spectrum of Ce cation.

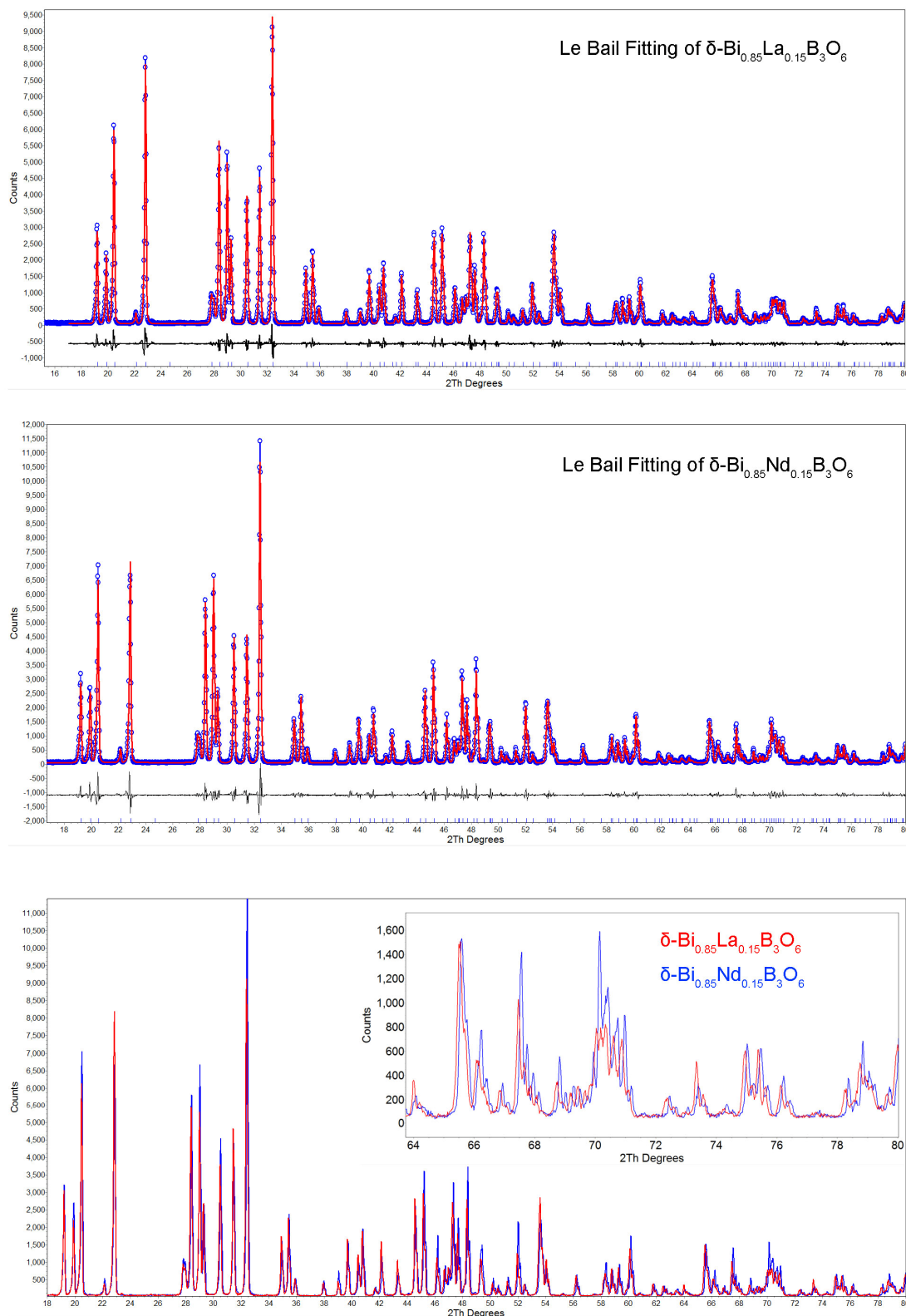


Figure S2. Le Bail fittings of two samples, $\delta\text{-Bi}_{0.85}\text{La}_{0.15}\text{B}_3\text{O}_6$ and $\delta\text{-Bi}_{0.85}\text{Nd}_{0.15}\text{B}_3\text{O}_6$ are quite good, and there is no sign of being multiphase for both samples. The first peak at low angle is not included during the refinements because the graphite monochromated XRD usually leads to strongly asymmetric peaks at low angle. These two samples possess the largest and the smallest cell volumes among all 28 samples

reported in our paper. The bottom figure shows the comparison of XRD patterns of above two samples (after the subtraction of the zero shifts). The peak positions, which reflect the cell lattice parameters, are not the same. This evidently shows that these two samples have different cell volumes but the difference is really small.

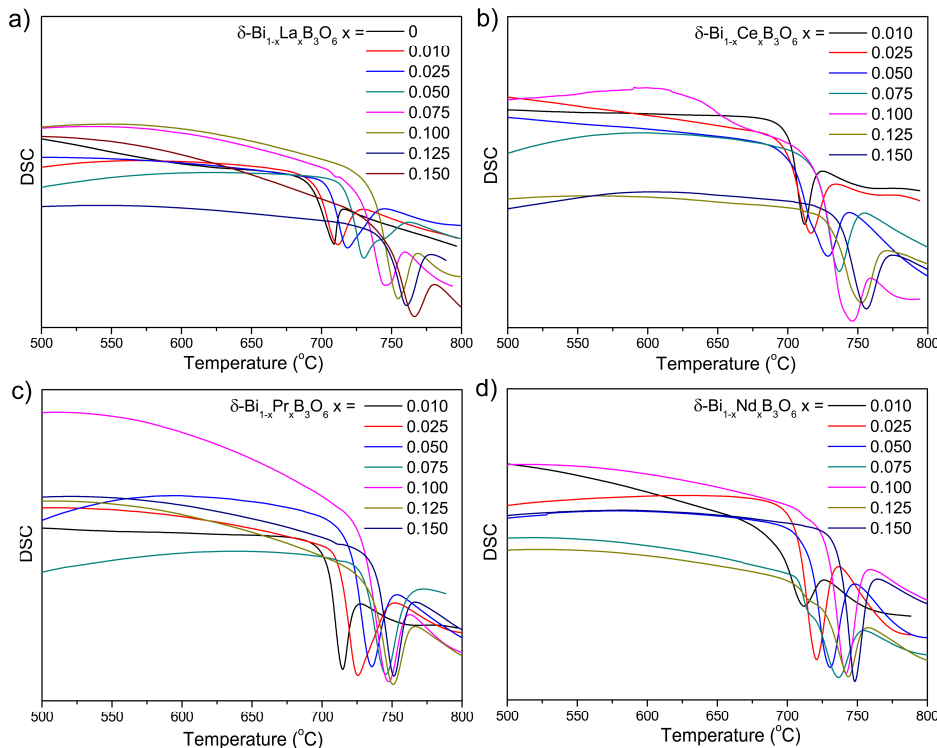


Figure S3. The DSC curves of the title samples. Only part of the curves (above 500 °C) is shown for clarity. Some of the curves are shifted upwards or downwards for better comparison.

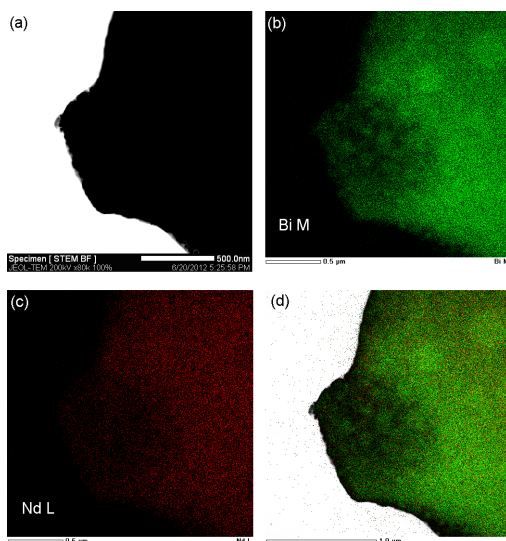


Figure S4. The TEM image of $\delta\text{-Bi}_{0.9}\text{Nd}_{0.1}\text{B}_3\text{O}_6$ (a) and its Bi/Nd distributions detected by EDX (b) Bi, (c) Nd. The right bottom figure is the overlay of Bi/Nd EDX results, which gives an atomic ratio of 91.52:8.48.

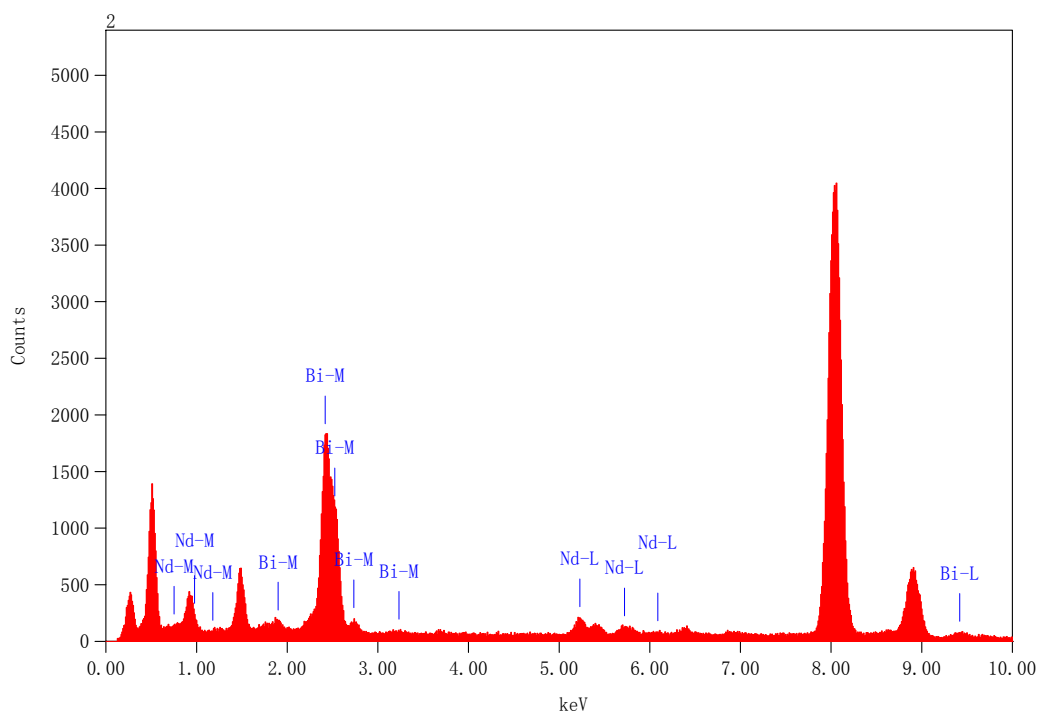


Figure S5. EDX analysis of $\delta\text{-Bi}_{0.9}\text{Nd}_{0.1}\text{B}_3\text{O}_6$.

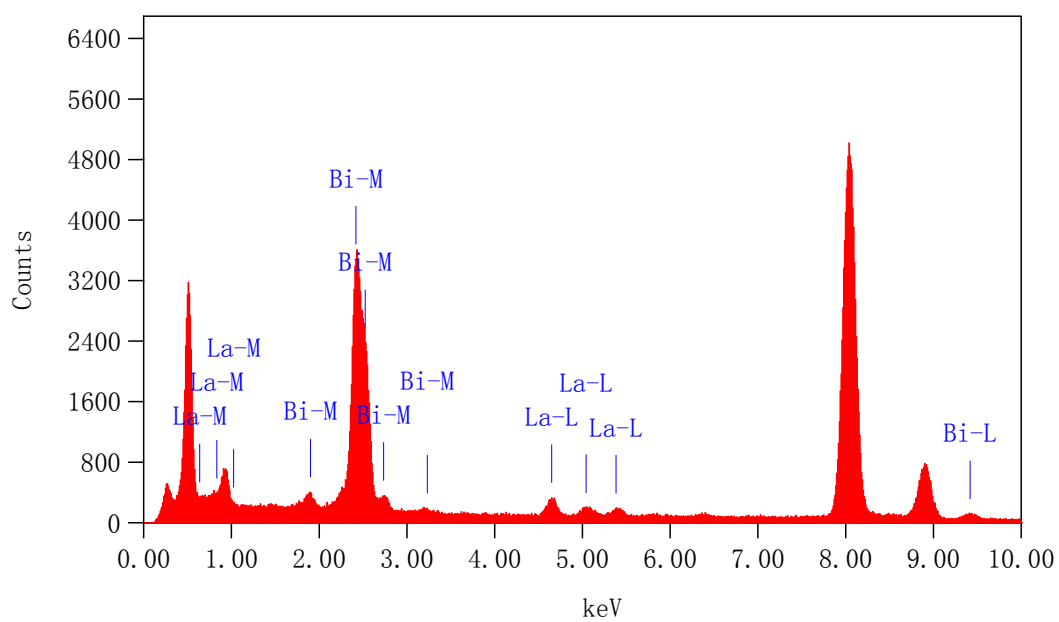


Figure S6. EDX analysis of $\delta\text{-Bi}_{0.9}\text{La}_{0.10}\text{B}_3\text{O}_6$.